

## Supporting Information

# Label-free LSPR Detection of Trace Lead(II) Ions in Drinking Water by Synthetic Poly(mPD-co-ASA) Nanoparticles on Gold Nanoislands

Guangyu Qiu<sup>a</sup>, Siu Pang Ng<sup>a</sup>, Xiongyi Liang<sup>a</sup>, Ning Ding<sup>b</sup>, Xiangfeng Chen<sup>b</sup>, Chi-Man Lawrence Wu<sup>a, b, \*</sup>

<sup>a</sup> *Department of Physics and Materials Science, City University of Hong Kong, Hong Kong SAR, P. R. China*

<sup>b</sup> *Shandong Academy of Science, Jinan, P.R. China*

Prof. Chi-Man Lawrence Wu

Tel: (+852) 34428668, Fax: (+852) 34420538, E-mail: apcmlwu@cityu.edu.hk

Department of Physics and Materials Science,

City University of Hong Kong,

Hong Kong SAR,

People's Republic of China

### Table of Contents

Figure S-1. Experimental set-up images and sensing diagram	S2
Figure S-2. Functionalization response of copolymer with various sizes	S3
Table S-1. Various ions and corresponding response compared to Pb(II)	S4
Table S-2. Comparison of different Pb(II) detection methods	S5
Figure S-3. Selectivity test results with Cu(II)-Fe(III)-Pb(II) mixture solution	S6
Figure S-4. Computational verification of possible repeat units of poly(mPD-co-ASA), and compare with experimental Raman spectrum.	S7
Figure S-5. Computational study of Pb(II) ions absorption on different functional groups.	S8
Table S-3. ICP-MS confirmation of Pb(II) in drinking water samples	S9
Reference	S9

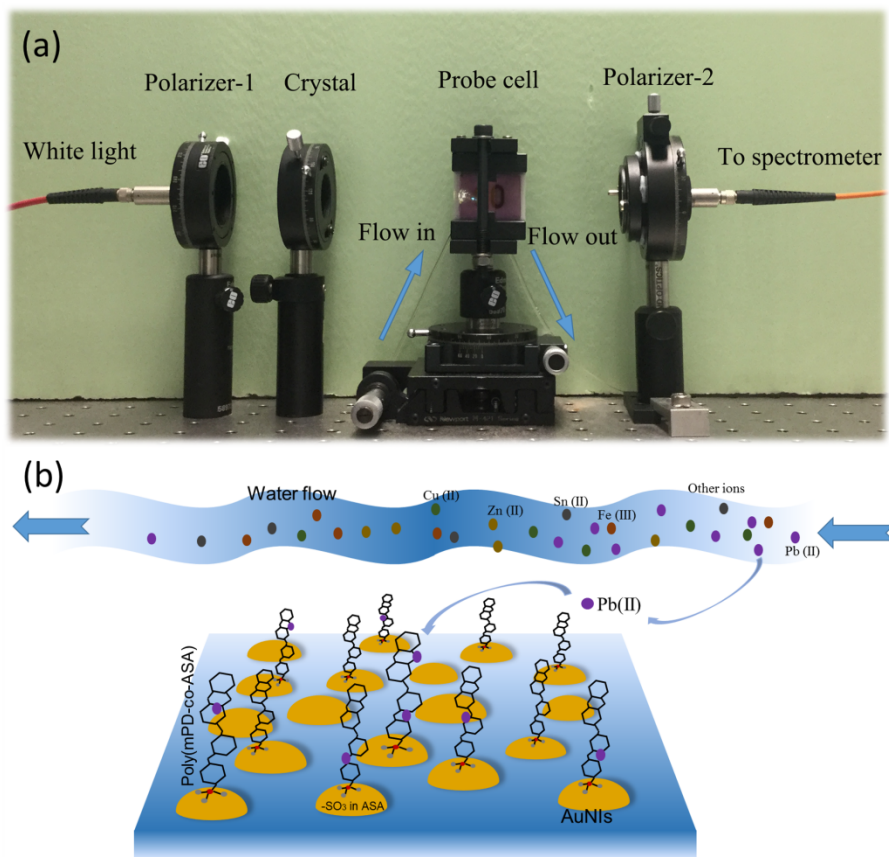


Figure S-1 (a) Experimental set-up for the detection of tracing Pb(II) in water. DW, copolymer solution and Pb(II) samples were injected through the flow-in tube of the probe cell. (b) Schematic representation of the mPD-co-ASA copolymer immobilized on gold surface, and the possible adsorption mechanism of Pb(II).

**Optical sensing system.** The common-path white light interferometric sensing system is introduced here. A white-light LED source (LedEngin, LZ1-00W00), with emission spectrum from 480 to 730 nm and bandwidth of 150 nm, was linearly polarized with a broadband polarizer (Edmund Optics, #89-602). A birefringent crystal (United Crystal, YVO4) was introduced into the light path so that sufficient retardation was introduced to the s-and p-polarized components. Then, the right-angle BK7 prism, as shown in supplementary Figure S-1a was used to couple the evanescent field of the incident light with the SAM-AuNIs on total internal reflection (TIR). This is similar to the Kretschmann SPR configuration and it was found that the TIR configuration produced higher extinction and better phase response than direct transmission for LSPR sensing with the SAM-AuNIs. In the whole process, the spectrometer (Advantes, Avaspec-ULS2048TEC) was used to record the total internal reflected interferometric spectrum and substantially processed with windows Fourier transform (WFT) to retrieve the differential phase.

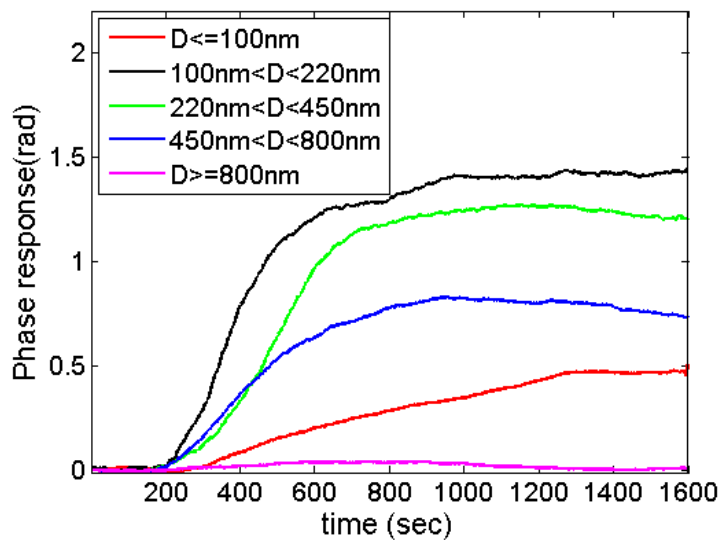


Figure S-2. Functionalization response of 95/5 poly(mPD-co-ASA) with five different particles diameter. The copolymer with particle size between 100nm to 220nm exhibited the best functionalization efficiency. However, when the particle size goes to higher than 800nm, after the flushing with DW water, the final phase response went back to approximate zero, which indicated the binding affinity was not strong enough to immobilized the large copolymer onto the AuNIs surface.

Table S-1 Suggested threshold ions concentration provided by WHO<sup>1</sup> and the corresponding differential phase response measured by poly(mPD-co-ASA) functionalized LSPR sensor.

Ions	Chemical formula	Concentration	Phase response	Selectivity ratio
Pb(II)	Lead(II) nitrate	10ppb	0.72	1
Cu(II)	Copper(II) sulfate	2ppm	0.0186	2.58333%
Al(III)	Aluminum(III) chloride	100ppb	0.086	11.9444%
Ni(II)	Nickel(II) chloride	70ppb	0.01452	2.016%
Cr(III)	Chromium (III) nitrate	50ppb	0.05012	6.961%
Ag(I)	Silver(I) nitrate	5ppb	0.0424	5.889%
Ba(II)	Barium (II) chloride	700ppb	0.03233	4.49%
Fe(III)	Iron(III) chloride	40ppm	0.034	4.7222%
Sn(II)	Tin(II) chloride	2ppb	0.0445	6.1805%
Mg(II)	Magnesium(II) chloride	20ppm	0.03789	5.2625%
Ca(II)	Calcium (II) acetate	80ppm	0.03859	5.360%
Na(I)	Sodium(I) chloride	20ppm	0.0215	2.98611%
K(I)	Potassium(I) chloride	10ppb	0.0456	6.333%
Zn(II)	Zinc(II) Nitrate	3ppm	0.02358	3.275%
Hg(II)	Mercury (II) chloride	6ppb	0.0112	1.555%
Cd(II)	Cadmium (II) nitrate	3ppb	0.02166	3.01%
Au(III)	Gold (III) chloride	10ppb	0.0226	3.138%
Cl <sup>-</sup>	Hydrochloric acids	10ppb	0.0093	1.29%
NO <sub>3</sub> <sup>-</sup>	Sulfuric acid	10ppb	0.0063	0.87%
SO <sub>4</sub> <sup>2-</sup>	Nitric acid	10ppb	0.0076	1.056%

Table S-2. Comparison between different Pb(II) detection methods for water samples.

Detection Methods	Synthesized Pb(II) receptors	LOD	Lifetime	Dynamic range	Reference
Electrochemical MOF	DNA functionalized MOF	0.007ppb	-	0.01ppb-41.4ppb	L. Cui, et al. <sup>2</sup>
Luminescence methods	G-quadruplex-selective iridium(III) complex	0.12ppb	-	0-0.518ppb	H. He, et al. <sup>3</sup>
Potentiometric methods	Semiconducting polymer microparticle	58.3ppb	5 months	65.4ppb-2606ppm	M. Huang, et al. <sup>4</sup>
Potentiometric methods	Copolymaniline nanoparticle in plasticizer-free membrane	0.005 ppb	15 months	207 ppm~0.021 ppb	X. Li, et al. <sup>5</sup>
Potentiometric methods	Polysulfoaminoanthraquinone Solid Ionophore	33.2 ppb	5 months	5200ppm-104 ppb	M. Huang et al. <sup>6</sup>
Colorimetric methods	Gold nanoparticle and DNAzyme	0.621ppb	-	0.621ppb-207ppb	Z. Wang, et al. <sup>7</sup>
Fluorescence methods	Selective Catalytic DNA	2.07ppb	-	2.07ppb-828ppb	J. Li, et al. <sup>8</sup>
Resonance light scattering	Dithiocarbamate-capped silver nanoparticles	0.828ppb	-	2.07ppb-12.4ppm	H. Cao, et al. <sup>9</sup>
SPR spectroscopy	Cross-linked chitosan thin film	0.5ppm	-	0.5ppm-100ppm	Y. Fen, et al. <sup>10</sup>
LSPR	gold nanoparticle-modified optical fiber	0.27ppb	-	10ppb-100ppb	T. Lin, et al. <sup>11</sup>
LSPR	Copolymer functionalized AuNIs	0.011ppb	5 months	0.011ppb-5ppm	Present work

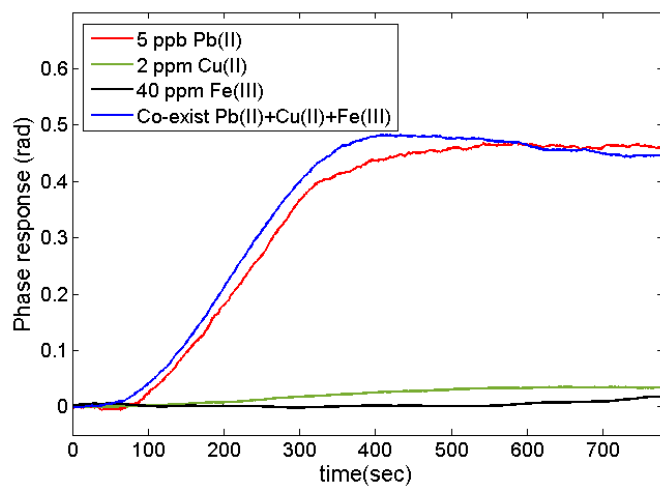


Figure S-3. Phase responses of the LSPR interferometric sensor to 200 ppm Cu(II), 40 ppm Fe(III), 5 ppb Pb(II) and combination of the three ions. Cu(II) and Fe(III) solution did not cause obvious phase response even though the concentration is thousands of times higher than that of Pb(II) in water. Also, the mixture solution of Cu(II) Fe(III) and Pb(II) produced similar phase response as that of Pb(II) only.

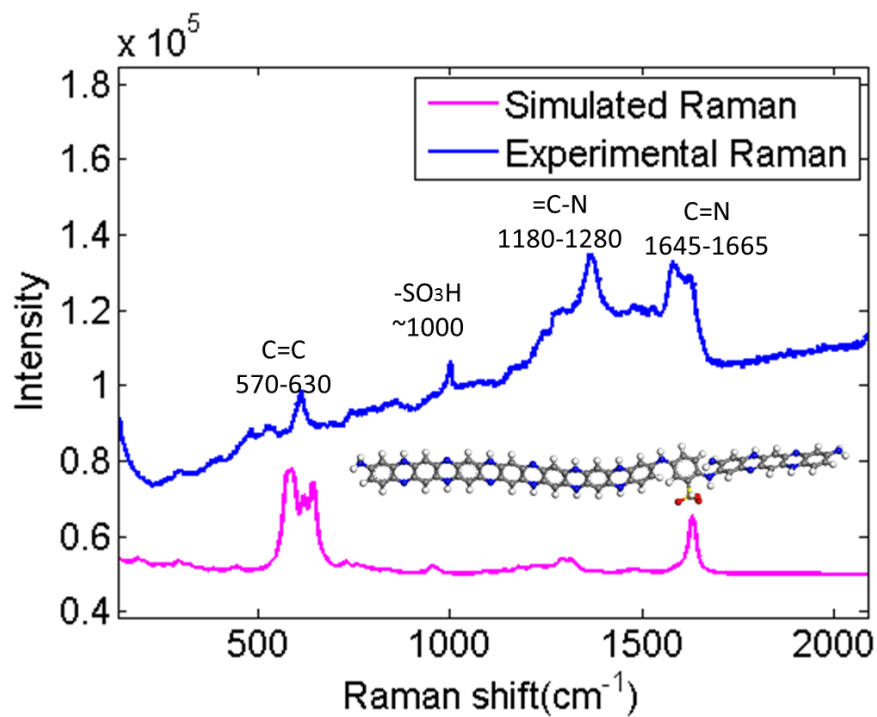
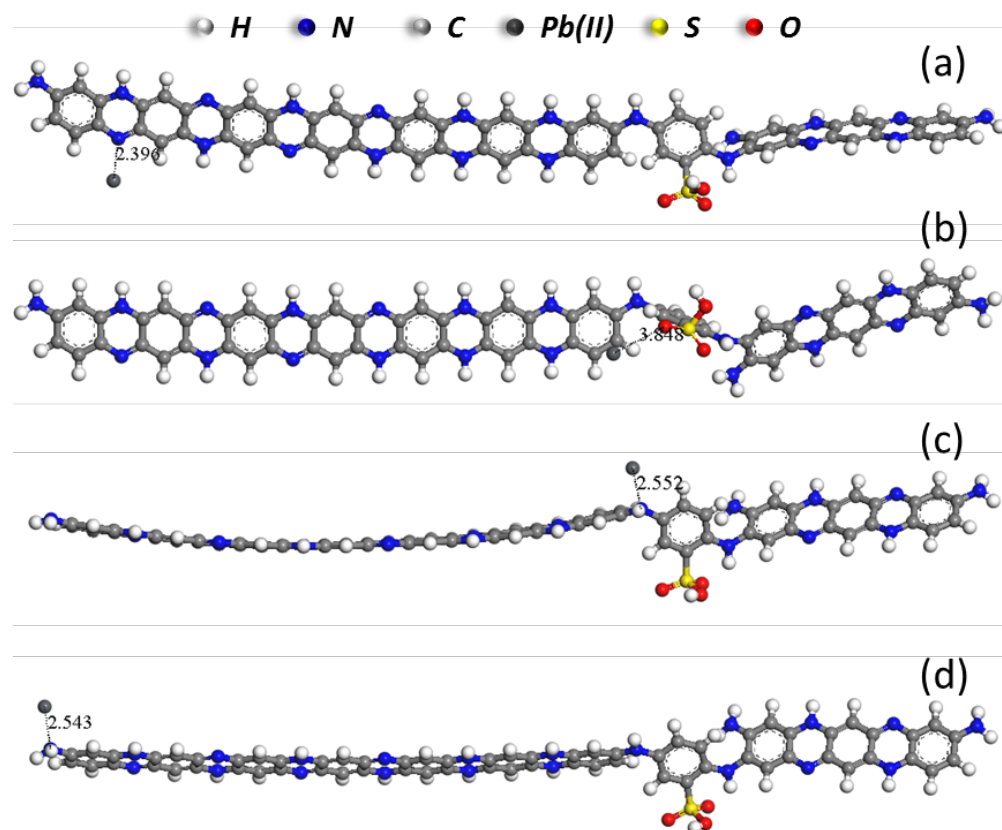


Figure S-4 Verification of possible repeat units of poly(mPD-co-ASA). The simulation Raman vibrational frequency (pink curve) showed good matching with Raman spectrum of as-synthesized copolymer.



Functional groups	Adsorption energy	Atoms Separation
-N=	-1.920615987 eV	2.396 Å
-SO <sub>3</sub> <sup>-</sup>	-1.52443433 eV	3.848 Å
-NH-	-1.526254772 eV	2.552 Å
-NH <sub>2</sub>	-1.667375814 eV	2.543 Å

Figure S-5. DFT simulation of Pb(II) adsorption onto possible poly(mPD-co-ASA) single repeating unit. The Pb(II) adsorption energy were calculated at (a) -N= group, (b) -SO<sub>3</sub><sup>-</sup> group, (c) -NH- group as well as (d) -NH<sub>2</sub> group. The corresponding adsorption energy were recorded into the table below the diagram. The results strongly suggested the -N= has the highest adsorption energy toward Pb(II), and other various functional groups also shown good adsorption to Pb(II).

For the adsorption systems, the adsorption energy is defined as

$$E_{ad} = E_{polymer+cation} - (E_{polymer} + E_{cation})$$

where  $E_{(polymer+cation)}$  is the energy of the optimized structure of pb<sup>2+</sup> adsorbed on polymer,  $E_{polymer}$  is the energy of isolated polymer, and  $E_{cation}$  is the energy of pb<sup>2+</sup>.

Table. S-3 ICP-MS confirmation of Pb(II) in tap water samples

Tap water samples	Poly(mPD-co-ASA) functionanlizied LSPR sensor	ICP-MS confirmation
Sample_1	1.11 ppb	0.80 ppb
Sample_2	14.0 ppb	14.32 ppb

## References

- (1) *Guideline for drinking-water qualities: recommendation*. World Health Organization: **2011**.
- (2) Cui, L.; Wu, J.; Li, J.; Ju, H. X. *Anal. Chem.* **2015**, *87*, 10635-10641.
- (3) He, H.-Z.; Leung, K.-H.; Yang, H.; Chan, D. S.-H.; Leung, C.-H.; Zhou, J.; Bourdoncle, A.; Mergny, J.-L.; Ma, D.-L. *Biosens. Bioelectron.* **2013**, *41*, 871-874.
- (4) Huang, M.-R.; Ding, Y.-B.; Li, X.-G.; Liu, Y.; Xi, K.; Gao, C.-L.; Kumar, R. V. *ACS Appl. Mater. Interfaces* **2014**, *6*, 22096-22107.
- (5) Li, X. G.; Feng, H.; Huang, M. R.; Gu, G. L.; Moloney, M. G. *Anal. Chem.* **2012**, *84*, 134-140.
- (6) Huang, M. R.; Ding, Y. B.; Li, X. G. *Acs Combinatorial Science* **2014**, *16*, 128-138.
- (7) Wang, Z.; Lee, J. H.; Lu, Y. *Adv. Mater.* **2008**, *20* (17), 3263-3267.
- (8) Li, J.; Lu, Y. *J. Am. Chem. Soc.* **2000**, *122*, 10466-10467.
- (9) Cao, H. Y.; Wei, M. H.; Chen, Z. H.; Huang, Y. M. *Analyst* **2013**, *138*, 2420-2426.
- (10) Fen, Y. W.; Yunus, W. M. M.; Talib, Z. A. *Optik* **2013**, *124*, 126-133.
- (11) Lin, T.-J.; Chung, M.-F. *Sensors* **2008**, *8*, 582-593.